Statistical distribution of the storm-time proton ring current: POLAR measurements

Y. Ebihara,[1] M. Ejiri,[1] H. Nilsson,[2] I. Sandahl,[2] A. Milillo,[3] M. Grande,[4] J. F. Fennell,[5] and J. L. Roeder[5]

Received 4 May 2002; revised 11 July 2002; accepted 28 August 2002; published 23 October 2002.

[1] Equatorial proton energy densities in the ring current region have been statistically investigated by compiling data acquired with the POLAR/MICS instrument (1–200 keV) in terms of the storm phases and Dst levels. The energy density is found to increase with decreasing Dst and to exhibit strong local time dependence during the storm main phase. In particular, the energy density at noon is interestingly shown to decrease during the main phase and increase during the recovery phase. A numerical simulation, which traces drift trajectories of the plasma sheet protons in the Volland-Stern type convection electric field, gives a reasonable result in comparison with the statistically obtained distribution. Those results support the scenario that the prime source of the higher energy density of the ring current protons is the plasma sheet protons whose drift motion is governed by the large-scale convection electric field most likely driven by the solar wind and IMF. *INDEX TERMS:* 2788 Magnetospheric Physics: Storms and substorms; 2730 Magnetospheric Physics: Magnetosphere—inner; 2753 Magnetospheric Physics: Numerical modeling; 2720 Magnetospheric Physics: Energetic particles, trapped. **Citation:** Ebihara, Y., M. Ejiri, H. Nilsson, I. Sandahl, A. Milillo, M. Grande, J. F. Fennell, and J. L. Roeder, Statistical distribution of the storm-time proton ring current: POLAR measurements, *Geophys. Res. Lett.*, *29*(20), 1969, doi:10.1029/2002GL015430, 2002.

1. Introduction

[2] Magnetospheric storms are known to be a consequence of the enhancement of energy density (ED) which is dominated by energetic ions with energy ranging between 10 keV and 120 keV in the inner magnetosphere [*Smith and Hoffman*, 1973; *Williams*, 1981]. Those energetic ions generate a large-scale electric current, called the ring current, that induces magnetic fields on the ground. The resultant magnetic field appears in the Dst index. Therefore the development and decay of the ED are a key in understanding the storm-time variation of Dst and its association with the ring current.

[3] Observations have shown that the ED enhancement is highly dependent on local time. Data from VIKING/MICS show large asymmetry of the ED between evening and morning local times at L of 4 for a storm [*Stüdemann et al.*, 1987]. On the basis of statistical analysis, *Greenspan and Hamilton* [2000] have shown that the majority of the ring current ED is on the night side and that less is in the morning-noon quadrant. *Korth et al.* [2000] reported a delay of the ED enhancement in the morning sector for >30 keV ions in comparison with that in the evening sector in a storm.

[4] No statistics have been given to exhibit the ED distribution in the ring current region except for the work done by *De Michelis et al.* [1999]. They averaged two years of proton data (1–300 keV) from AMPTE CCE/CHEM to show the equatorial plasma pressure distribution for different AE levels; AE < 100 nT for "quiet" and 100 < AE < 600 nT for "active". No substantial difference between them is shown in their result, likely meaning that the equatorial pressure of ring current protons is, according to their result, independent of the AE levels that they defined.

[5] We compiled proton data from POLAR to "visualize" the proton ED distribution in the inner magnetosphere ($L \leq 8$). To our knowledge, this is the first statistical distribution of the proton ED distribution (proton ring current) in terms of storm development.

2. Data

[6] POLAR was launched on February 24, 1996 into an elliptic orbit with perigee of 2 R_E and apogee of 9 R_E at $\sim 86°$ inclination.The Charge and Mass Magnetospheric Ion Composition Experiment/Magnetospheric Ion Composition Sensor (CAMMICE/MICS) aboard the POLAR satellite has measured the ion count rates, mass, and charge state in the energy range of 1–200 keV/q [*Wilken et al.*, 1992].

[7] To minimize uncertainty due to the off-equatorial measurements,we used data measured near the equatorial plane with the criterion that $B/B_0 \leq 1.2$, where B and B_0 are the magnetic field at the satellite position and the minimum magnetic field along the field line. The magnetic latitude where $B/B_0 = 1.2$ is $\pm 12°$ if the magnetic field is a dipole. The magnetic fields, B and B_0, were calculated with IGRF and the Kp-dependent external field model of T89c [*Tsyganenko*, 1989]. The input parameter for the T89c model was kept constant at the lowest level in Kp, that is, Kp = 0. We believe that the result is not sensitive to the input parameter assumed because we deal with the near-equatorial data.

[8] A total of 28850 available proton spectra were selected for the period between March 6, 1997 and March 13, 2000 and were integrated over the energy range between 1 and 200 keV to calculate the ED.

3. Results

3.1. Storm Phase Dependence

[9] In this particular study, we defined the storm main and recovery phases by the following criteria. *The main*

[1]National Institute of Polar Research, Tokyo, Japan.
[2]Swedish Institute of Space Physics, Kiruna, Sweden.
[3]Istituto di Fisica dello Spazio Interplanetario, Roma, Italy.
[4]Rutherford Appleton Laboratory, Chilton, Didcot, United Kingdom.
[5]The Aerospace Corporation, Los Angeles, California, USA.

0094-8276/02/2002GL015430$05.00

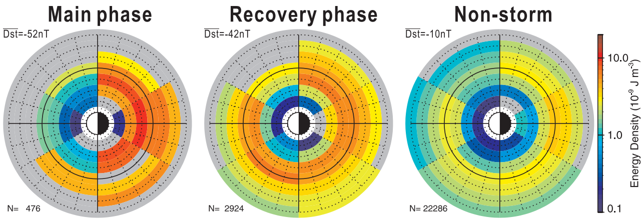

Figure 1. Dial plots of ED in the L-MLT coordinates ($L \leq$ 8) sorted by storm phases; main (left),recovery (middle), and non-storm time (right).The ED is coded by colors. The solid circle indicates L = 5, and the sun is to the left.

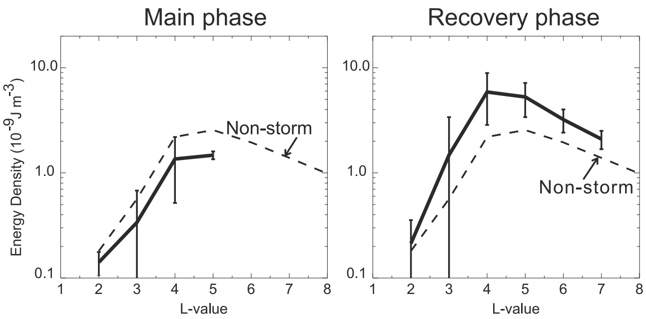

Figure 2. Cross section of the ED at magnetic noon for the storm main phase (left)and the storm recovery phase (right). The non-storm time ED is indicated by a dashed line. Vertical bars indicate the standard deviation.

phase starts with a sudden decrease in Dst, followed by a subsequent decrease down to −50 nT or less. The main phase lasts until the recovery phase commences. *The recovery phase* starts with Dst turning to decrease, and lasts two days. Storms that were accompanied by sawtooth fluctuation in Dst were removed from the data set because the main and recovery phases of such storms are not simply identified.

[10] The result is shown in Figure 1. In the main phases the ED enhancement is prominent in the night and evening sectors. The ED reaches a peak of 10 nJm^{-3} at L = 4 at midnight, but in contrast, it reaches a peak of only 1.5 nJm^{-3} at L = 5 at noon. In the recovery phases the ED in the 0600–1400 MLT sector starts to increase and the ED distribution approaches uniformity; 6 nJm^{-3} (midnight) and 5 nJm^{-3} (noon) at L = 5. Figure 2 shows the cross section of the ED at magnetic noon. The ED at noon during the main phase is interestingly shown to be less than in the non-storm time ED. The ED at noon starts to increase in the recovery phase, and exceeds the non-storm time ED. This is most likely attributed to sudden decrease in the convection electric field [*Hultqvist et al.*, 1981].

[11] *Greenspan and Hamilton* [2000] found that the dayside measurements of the total ED do not show a robust correlation with Dst while there is a strong linear correlation between the nightside measurement of the total energy and Dst. Their result is consistent with our result that the dayside ED enhancement is obscure during the storm main phase while the nightside one is obviously enhanced.

3.2. Dst Dependence

[12] The ED distributions sorted by different Dst levels are shown in the top panels of Figure 3. The dial plots exhibit a clear tendency that the maximum ED increases and its L-value shifts inward with decreasing Dst. For example, the ED maxima are 3, 6, 10, and 14 nJm^{-3} at midnight for Dst levels of 0 to −30, −30 to −60, −60 to −90 and <−90 nT, respectively.

[13] We performed a numerical simulation [c.f., *Ebihara and Ejiri*, 2000] to demonstrate how a basic process of physics governs the observed effect. The distribution function which was assumed to be isotropic at L = 9 was given by an empirical model of the equatorial proton distribution function based on AMPTE/CCE/CHEM data for AE < 100 nT [*Millilo et al.*, 2001], and the bounce-averaged trajectories were traced in the dipole magnetic field and the Volland-Stern type convection electric field with a shielding factor of 2. The averaged polar cap potential drops summarized in Table 1 were used, and they were kept constant throughout the calculation. The other parameters were held constant. It seems crude to trace particle motion under the simplified field models. However, to the zeroth order approximation, they are reasonable, or not so far from the reality for the purpose to find a significant parameter primarily governing the ring current.

[14] The bottom panels of Figure 3 show snapshots of the calculated ED at elapsed time of 12 hours when the incoming and outgoing particles are close to be balanced, suggesting that the plasma sheet protons convecting toward dayside are primarily responsible for the ED development. A discrepancy is found in the early morning sector (0200–0600 MLT), that is, the observed ED is further extended from nightside toward morning sector. This discrepancy is most likely attributed to the electric field model that we assumed. The realistic convection electric field model based on ionospheric electric field measurements [e.g., *Weimer*, 1996] is known to give better agreement with observed ion spectra than the Volland-Stern type model [*Kistler and Larson*, 2000; *Jordanova et al.*, 2001]. We intend to emphasize that the overall enhancement of the ED is primarily due to the enhancement of the convection electric field rather than the shape of the convection electric field. This was pointed out by *Liemohn et al.* [2001]. The plasma sheet density is suggested to be one of the dominant sources of the ring current development [e.g., *Kozyra et al.*, 1998; *Ebihara and Ejiri*, 2000]. However, the result shows that on

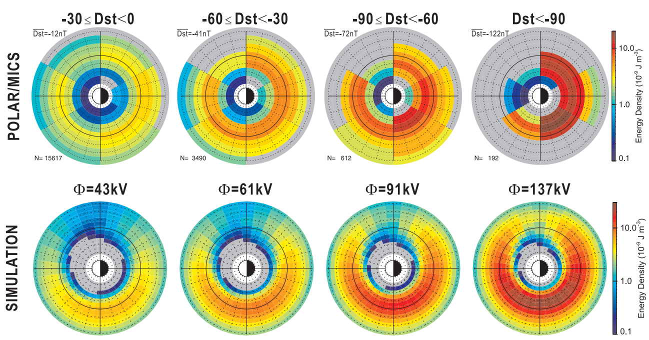

Figure 3. (top) Same as Figure 1 except for those sorted by different Dst levels, from left to right, −30 ≤ Dst < 0, −60 ≤ Dst < −30, −90 ≤ Dst< −60,and −90 < Dst. (bottom) Simulated ED at the elapsed time of 12 hours from the beginning of the simulation. From left to right.

Table 1. Averaged Dst* and Dst*(DPS) for Different Dst Levels

Dst level	*N*	$\overline{\text{Dst*}}$	Dst*(DPS)	$\overline{\Phi_{PCP}}$
$-30 \leq$ Dst < 0	15617	−15 nT	−21 nT	43 kV
$-60 \leq$ Dst < −30	3490	−45 nT	−29 nT	61 kV
$-90 \leq$ Dst < −60	612	−79 nT	−43 nT	91 kV
−90 < Dst	192	−135 nT	−53 nT	137 kV

The averaged polar cap potential drop Φ_{PCP} was calculated with the help of the empirical model given by *Boyle et al.* [1997].

the average the role of the plasma sheet density in the ring current development is not clearly seen (figure not shown). This is simply understood that the averaged plasma sheet density gives the averaged ED distribution of the ring current.

[15] Next we examine how much the proton ring current contributes to the Dst depression associated with magnetic storms. The most appropriate scheme is to evaluate the Dst value with the help of the DPS relation [*Dessler and Parker*, 1959; *Sckopke*, 1966]. By assuming that the ED distribution is uniform along a field line, a crude accumulation of the ED was performed to obtain the total energy as T. E. = $\int \epsilon(L, \phi)dV$, where ϵ is the ED, ϕ is MLT, and dV is the volume element of unit L and ϕ in the dipole coordinates as

$$dV = 2a^3L^2\sqrt{1-\frac{1}{L}}\left(\frac{1}{7L^3}+\frac{6}{35L^2}+\frac{8}{35L}+\frac{16}{35}\right)dLd\phi, \quad (1)$$

where a is the earth's radius. The effect of the earth's induction, which is assumed to enhance Dst by 50%, was introduced into the calculation. In contrast with previous studies [e.g., *Lui et al.*, 1987; *Hamilton et al.*, 1988; *Roeder et al.*, 1996; *Greenspan and Hamilton*, 2000], the spatial distribution (L and MLT) of the ED is taken into account to calculate the total energy in the ring current region. Hereinafter, the calculated magnetic field is denoted by Dst* (DPS).

[16] Unfortunately, all the L and MLT bins that we are interested in ($L < 8$) were not fully covered by POLAR. The missing bins(indicated by the gray color in Figure 3) were made up for by the available energy densities averaging over the same L-value. As for the lowest Dst level (Dst < −90), no available data are found at L = 8 in any of the MLTs. We adapt the empirical ED given by *Spence and Kivelson* [1993] into these particular bins.

[17] The result is summarized in Table 1. Dst* stands for the Dst corrected by subtracting the contribution from the magnetopause current as $\text{Dst*} = \text{Dst} - bP_{sw}^{1/2} + c$, where P_{sw} is the dynamic pressure of the solar wind, and b and c are the empirical coefficients, respectively. The coefficients, b and c, are known to be typically 0.2 nT/(eV cm^{-3})$^{1/2}$ and 20 nT, respectively [e.g., *Gonzalez et al.*, 1994].

[18] If the Dst* was induced solely by the proton ring current, the two Dst* values, $\overline{\text{Dst*}}$ and Dst*(DPS), would be the same. However, the two Dst* values tend to show disagreement for stronger storms (Dst < −60 nT).This is not a surprising result because other species and other current systems are expected to contribute to Dst* for stronger storms. The contribution from electrons to Dst is estimated to be 20% of the ion ED [*Frank*, 1967], and the contribution from the oxygen ions to be ~20% to the total ion ED for small or moderate storms [*Daglis*, 1997]. This provides a crude estimate that the total plasma energy gives−65 nT ($-90 \leq$ Dst < −60) and −106 nT (−90 < Dst) in Dst*, and they correspond to 80% of the observed Dst*, respectively. One may attribute the remain (20% of total) to the contribution from the tail current [*Ohtani et al.*, 2001]. However, we cannot reach a general conclusion unless we investigate the other contributions (oxygen ions, electrons, higher energy ions) to Dst* definitely.

4. Implications

[19] The statistical distribution of the proton ring current revealed the following characteristic: The ED in the 0600–1400 MLT sector decreases during the storm main phase, and increases and approaches uniformity in the recovery phase. This characteristic, which has been predicted by numerical simulations [e.g., *Kozyra et al.*, 1998; *Ebihara and Ejiri*, 2000], likely supports the following scenario that has been widely thought to occur during storms:

1. Southward component of IMF and high-speed solar wind enhances the large-scale convection electric field.
2. When the convection electric field is enhanced, plasma sheet protons drift earthward deeply, and are energized adiabatically. Consequently, they contribute to enhancement of the ED in the evening-night sector.
3. When the convection electric field is weakened, most protons become trapped, and consequently, the ED distribution approaches uniformity in MLT. Some of them are possible to escape from the dayside magnetopause.
4. Trapped protons are lost by some loss processes.

[20] The existence of the ED minima around the prenoon region during the main phase suggests that the convection electric field during the main phase is rather "DC-like". If the convection electric field fluctuates drastically in short time, (for example with amplitudes up to 100 kV), the ED would increase at all MLT during the storm main phase because the above processes between item "2" and item "3" are repeated [*Chen et al.*, 1994]. The ED minima would be filled with ions coming from the dusk region within a half of drift period (~7 hours for 10 keV and ~40 minutes for 100 keV at L = 5) which is shorter than typical duration of a storm main phase (~12 hours or more). Our result, however, does not rule out the possibility that the "AC-like" electric field contributes to the storm-time development of the ED because our study is based on statistics.

[21] We have to discuss the contribution from higher energy protons (>200 keV) that are not measured by MICS. On the basis of the Explorer 45 data, *Smith and Hoffman* [1973] have shown that the higher energy ions (300–872 keV) dominate the quiet-time ring current at L < 4. *Lui et al.* [1994] evaluated the possibility that the high energy ions dominate the plasma pressure at $L < 4$, and they found that the >872 keV ions contribute typically ~50–65% to the plasma pressure at L < 4 for quiet periods. Their plasma pressure profile, which is calculated from ions in the energy range between 1 keV and 4MeV, exhibits the peak L of around 3.0–3.5 [*Lui and Hamilton*, 1992]. In contrast with this, the ED calculated from protons in the energy range of 1–200 keV peaks at L = 5–6 during quiet time (Dst $\geq$ 0, not shown). This difference is most likely attributed to the energy range used.

[22] As for active periods, *Smith and Hoffman* [1973] have shown that the high energy portion of the ion ED

(300–872 keV) was depleted and only contributed 19% to the total proton ED at $L = 3$ during the magnetic storm of December 1971, that is, such high energy ions are probably regarded as a lesser contributor and/or as "back-ground" to the storm-time ring current. This tendency has also been seen in data from Explorer 45 [*Lyons and Williams*, 1976], ISEE 1 [*Williams*, 1981] and CRRES [*Fu et al.*, 2001]. Investigation of the behavior of the high energy ions is needed to understand the overall dynamics of the storm-time ring current development.

[23] We have to keep in mind that all of the results come from statistical analysis. This means that we cannot say anything about the temporal evolution of the ED. Global and instantaneous imaging of the ring current particles through energetic neutral atoms (ENAs) [e.g., *Mitchell et al.*, 2001] could be a powerful tool for investigating the temporal development of the ED.

[24] **Acknowledgments.** We are grateful to T. A. Fritz, PI of POLAR/CAMMICE, and B. Kellett for the arrangement and technical suggestions for the use of the MICS database. Y. E. gratefully acknowledges discussion with N. Yu. Ganushkina. The solar wind parameters were obtained through the OMNI database. The Dst index was provided from the World Data Center for Geomagnetism, Kyoto.

References

Boyle, C. B., P. H. Reiff, and M. R. Hairston, Empirical polar cap potentials, *J. Geophys. Res.*, *102*, 111, 1997.

Chen, M. W., L. R. Lyons, and M. Schulz, Simulations of phase space distributions of storm time proton ring current, *J. Geophys. Res.*, *99*, 5745, 1994.

Daglis, I. A., The role of magnetosphere-ionosphere coupling in magnetic storm dynamics, in *Magnetic Storms*, *Geophys. Monogr. Ser.*, vol. 98, edited by B. T. Tsurutani, W. D. Gonzalez, Y. Kamide, and J. K. Arballo, pp. 107, AGU, Washington, D. C., 1997.

Dessler, A. J., and E. N. Parker, Hydrodynamic theory of geomagnetic storms, *J. Geophys. Res.*, *64*, 2239, 1959.

De Michelis, P., I. A. Daglis, and G. Consolini, An average image of proton plasma pressure and of current systems in the equatorial plane derived from AMPTE/CCE-CHEM measurements, *J. Geophys. Res.*, *104*, 28,615, 1999.

Ebihara, Y., and M. Ejiri, Simulation study on fundamental properties of the storm-time ring current, *J. Geophys. Res.*, *105*, 15,843, 2000.

Fu, S. Y., et al., Ion composition variations in the inner magnetosphere: Individual and collective storm effects in 1991, *J. Geophys. Res.*, *106*, 29,683, 2001.

Frank, L. A., On the extraterrestrial ring current during geomagnetic storms, *J. Geophys. Res.*, *72*, 3753, 1967.

Gonzalez, W. D., J. A. Joselyn, Y. Kamide, H. W. Kroehl, G. Rostoker, B. T. Tsurutani, and V. M. Vasyliunas, What is a geomagnetic storm?, *J. Geophys. Res.*, *99*, 5771, 1994.

Greenspan, M. E., and D. C. Hamilton, A test of the Dessler-Parker-Sckopke relation during magnetic storms, *J. Geophys. Res.*, *105*, 5419, 2000.

Hamilton, D. C., et al., Ring current development during the great geomagnetic storm of February 1986, *J. Geophys. Res.*, *93*, 14,343, 1988.

Hultqvist, et al., Decrease of keV electron and ion fluxes in the dayside magnetosphere during the early phase of magnetospheric disturbances, *J. Geophys. Res.*, *29*, 107, 1981.

Jordanova, V. K., et al., Effects of inner magnetospheric convection on ring current dynamics: March 10–12, 1998, *J. Geophys. Res*, *106*, 29,705, 2001.

Kistler, L. M., and D. J. Larson, Testing electric and magnetic field models of the storm-time inner magnetospher, *J. Geophys. Res.*, *105*, 25,221, 2000.

Korth, A., et al., Comprehensive particle and field observations of magnetic storms at different local times from the CRRES spacecraft, *J. Geophys. Res.*, *105*, 18,729, 2000.

Kozyra, J. U., et al., Effects of a high-density plasma sheet on ring current development during the November 2–6 1993, magnetic storm, *J. Geophys. Res.*, *103*, 26,285, 1998.

Liemohn, M. W., et al., Dominant role of the asymmetric ring current in producing the storm time Dst*, *J. Geophys. Res.*, *106*, 10,883, 2001.

Lui, A. T. Y., and D. C. Hamilton, Radial profiles of quiet time magntospheric parameters, *J. Geophys. Res.*, *97*, 19,325, 1992.

Lui, A. T. Y., R. W. McEntire, and S. M. Krimigis, Evolution of the ring current during two geomagnetic storms, *J. Geophys. Res.*, *92*, 7459, 1987.

Lui, A. T. Y., H. E. Spence, and D. P. Stern, Empirical modeling of the quiet time nightside magnetosphere, *J. Geophys. Res.*, *99*, 151, 1994.

Lyons, L. R., and D. J. Williams, Storm-associated variations of equatorially mirroring ring current protons, 1–800 keV, at constant first adiabatic invariant, *J. Geophys. Res.*, *81*, 216, 1976.

Mitchell, D. G., et al., Imaging two geomagnetic storms in energetic neutral atoms, *Geophys. Res. Lett.*, *28*, 1151, 2001.

Millilo, A., et al., Empirical model of proton fluxes in the equatorial inner magnetosphere: Development, *J. Geophys. Res.*, *106*, 25,713, 2001.

Roeder, J. L., et al., CRRES observations of stormtime ring current ion composition, in *Workshop on the Earth's Trapped Particle Environment*, AIP Conf. Proc., 383, pp. 131, 1996.

Ohtani, S., et al., Storm-substorm relationship: Contribution of the tail current to Dst, *J. Geophys. Res.*, *106*, 21,199, 2001.

Sckopke, N., A general relation between the energy of trapped particles and the disturbance field near the earth, *J. Geophys. Res.*, *71*, 3125, 1966.

Smith, P. H., and R. A. Hoffman, Ring current particle distributions during the magnetic storms of 16–18 December 1971, *J. Geophys. Res.*, *78*, 4731, 1973.

Spence, H. E., and M. G. Kivelson, Contributions of the low-latitude boundary layer to the finite width magnetotail convection model, *J. Geophys. Res.*, *98*, 15,487, 1993.

Stüdemann, et al., The May 2–3, 1986 magnetic storm: First energetic ion composition observations with the MICS instrument on Viking, *Geophys. Res. Lett.*, *14*, 455, 1987.

Tsyganenko, N. A., A magnetospheric magnetic field model with a warped tail current sheet, *Planet. Space Sci.*, *37*, 5, 1989.

Weimer, D. R., A flexible, IMF dependent model of high-latitude electric potentials having "space weather" applications, *Geophys. Res. Lett.*, *23*, 2549, 1996.

Wilken, B., et al., Magnetospheric ion composition spectrometer onboard the CRRES spacecraft, *Journal of Spacecraft and Rockets*, *29*, 585, 1992.

Williams, D. J., Ring current composition and sources: An update, *Planet. Space Sci.*, *29*, 1195, 1981.

Y. Ebihara and M. Ejiri, National Institute of Polar Research, 1-9-10 Kaga, Itabashi-ku, Tokyo 173-8515, Japan. (ebihara@nipr.ac.jp; ejiri@nipr.ac.jp)

H. Nilsson and I. Sandahl, Swedish Institute of Space Physics, Box 812, S-981 28, Kiruna, Sweden. (hane@irf.se; ingrid@irf.se)

A. Milillo, Instituto di Fisica dello Spazio Interplanetario, del Fosso del Cavaliere 100-00133, Roma, Italy. (Anna.Milillo@ifsi.rm.cnr.it)

M. Grande, Rutherford Appleton Laboratory, Chilton, Didcot, United Kingdom. (M.grande@rl.ac.uk)

J. F. Fennell and J. L. Roeder, The Aerospace Corporation, Los Angeles, California, USA. (joseph.f.fennell@aero.org; james.roeder@aero.org)